Dalton Transactions

Accepted Manuscript

This article can be cited before page numbers have been issued, to do this please use: Y. Guo, S. Song, Y. Zheng, R. Li and T. Peng, *Dalton Trans.*, 2016, DOI: 10.1039/C6DT01248E.

ROYAL SOCIETY OF CHEMISTRY

www.rsc.org/dalton

View Article Online
DOI: 10.1039/C6DT01248E

Journal Name

ARTICLE

Synthesis and characterization of A_2BC type phthalocyanine and its visible-light-responsive photocatalytic H_2 production performance on graphitic carbon nitride

Received 00th January 20xx,
Accepted 00th January 20xx

DOI: 10.1039/x0xx00000x

www.rsc.org/

Yingying Guo,[a] Shuaishuai Song,[a] Ya Zheng,[a] Renjie Li*[a] and Tianyou Peng*[a]

Highly asymmetric A_2BC type zinc phthalocyanine (Zn-*di*-PcNcTh) has been designed and synthesized. The Zn-*di*-PcNcTh used π electron rich thiophene ring in place of the benzenoid rings of phthalocyanine which was acting as electron donor, diphenylphenoxy substituents to retard aggregation and a carboxyl-naphthalene unit as electron acceptor. The asymmetric phthalocyaine shows a strongly Q-band split and wide spectral absorption in the visible/near-IR light region, which can extend the spectral response region of graphitic carbon nitride (g-C_3N_4) from ~450 nm to more than 800 nm. By using as a sensitizer of 1.0 wt% Pt-loaded graphitic carbon nitride (g-C_3N_4), the experimental results indicate that Zn-*di*-PcNcTh-Pt/g-C_3N_4, shows a H_2 production efficiency of 249 μmol h^{-1} with an impressive turnover number (TON) of 9960.8 h^{-1} under visible light (λ ≥ 420 nm) irradiation, much higher than that of the pristine Pt/g-C_3N_4. Owing to the introduction of highly bathochromic shift of 3,4-dicyanothiophenethe and valuable "push–pull" effect from thiophene (electron donor) to carboxyl-naphthalene (electron acceptor) unit, Zn-*di*-PcNcTh/g-C_3N_4 gives an extremely high apparent quantum yield (AQY) of 2.44%, 3.05%, 1.53% at 700, 730, 800 nm monochromatic light irradiation at optimized photocatalytic condition.

Introduction

During the past decades, increasing attention has been paid to the photocatalytic procedure for clean hydrogen energy production over semiconductor, due to the increasingly serious energy and environment crises.[1-4] Besides the commonly used semiconductors such as TiO_2 and CdS, graphitic carbon nitrides (g-C_3N_4) as a novel polymer semiconductor have attracted numerous attentions due to its specific planar structure, physicochemical property and appropriate energy band positions for photosplitting water.[5-7] The utilization of g-C_3N_4, opens up a new prospect to construct highly efficient and economical photocatalysis systems. However, the bandgap of g-C_3N_4 is 2.7 eV with an absorption edge just at ~ 450 nm, which largely restricts the utilization efficiency of visible-light.[8-10] To extend its visible light absorption and improve its photocatalytic activity, several strategies, such as doping with metal or nonmetallic elements,[11] copolymerization of two or more precursors,[12] surface modification[13,14] and dye sensitization[15,16] have been developed. Among various strategies for visible-light harvesting, dye sensitization is one of the efficient approaches to expand the spectral response region of semiconductors.

As the light harvesting center, the dye must possess certain essential requirements such as broad light response, appropriate redox potential for electron-injection and regeneration following light excitation, stability under long-term light irradiation and inexpensive. Typically, organic dyes (such as Eosin Y,[17] Rhodamine B[18] and coumarin dyes[19,20]) and metal complexes (such as Ru-complexs[3,21] and metal porphyrin[22]) are the most commonly used sensitizers in dye-sensitized semiconductors for H_2 production. However, ruthenium is a rare metal, and the embarrassing thing is that most common used dyes hardly extend the spectral response to longer than 600 nm. Phthalocyanines (Pcs) are planar 18 π-electron conjugated system, which generates intense absorption in the UV/blue (Soret B band) and the red/near-IR (Q-band) spectral regions. In addition, the excellent photochemical/thermal stabilities and appropriate redox properties of Pcs also render them attractive dye for the sensitization of wide-band-gap semiconductors such as TiO_2.[23,24] Dye sensitization of g-C_3N_4 is also an efficient way to use the visible light of solar radiation. Until now, poly(3-hexylthiophene) (P3HT), Erythrosin B (ErB) and Eosin Y (EY) are used as sensitizers for g-C_3N_4 to enhance the photocatalytic H_2 production activity with considerable visible-light utilization efficiency and maximal responsive wavelength at ~ 600 nm.[17,25,26] However, there was rare study of the utilization of huge visible/near-IR light with wavelength longer than 600 nm, Pc-sensitized g-C_3N_4 showed photocatalytic H_2 production activity. Domen *et al*. exploited MgPc-sensitized g-C_3N_4 for H_2 evolution, which showed photocatalytic H_2 production activity at 600-800 nm but with rather low apparent quantum yield (AQY) of 0.07% at ~ 660 nm.[15] Lu *et al*. reported that a MnPc covalently functionalized

[a] College of Chemistry and Molecular Sciences, Wuhan University, Wuhan 430072, P. R. China.

† Electronic Supplementary Information (ESI) available: [details of any supplementary information available should be included here]. See DOI: 10.1039/x0xx00000x

View Article Online
DOI: 10.1039/C6DT01248E

graphene nanohybrid (MnPc-G) photocatalyst showed photocatalytic hydrogen evolution at 600-800 nm and apparent quantum efficiency (0.06%) at 670 nm.[27] Therefore, the development of an efficient near-IR responsive catalyst still have a broad prospect.

Recently, highly conjugated mononaphthalo-triphthalocyanine derivatives (Zn-*tri*-PcNc) have been designed and synthesized by our group, which showed a Q-band redshift to the near-IR region stemmed from the expanded π-conjugated macrocycle by introducing an additional benzo group to the benzopyrrole groups of the ZnPc framework. Zn-*tri*-PcNc was used to sensitize TiO_2 for H_2 production, which showed a considerable photoactivity and 0.2% AQY at 700 nm monochromatic light.[24] When Zn-*tri*-PcNc was utilized as a sensitizer to extend the spectral response region of g-C_3N_4 from 450 nm to more than 800 nm. After optimizing the photocatalytic condition and adding chenodeoxycholic acid (CDCA) as coadsorbent, Zn-*tri*-PcNc sensitized g-C_3N_4 photocatalyst showed a H_2 production efficiency of 125.2 μmol h^{-1} under visible-light irradiation and 1.85% apparent quantum yield (AQY) at 700 nm monochromatic light irradiation, improved by 50.5% compared with the photoreaction system without CDCA.[4] It indicated that the steric hindrance of the three *tert*-butyl groups in Zn-*tri*-PcNc is too small to effectively retard phthalocyanine π-π stacking, while the aggregation tendency of ZnPc is considered to enhance the self-quenching of the dye excited singlet state, thus resulting in decreased efficiency. To enhance the steric hindrance, Zn-*tri*-PcNc-8 has been synthesized with six diphenylphenoxy to suppress the molecular aggregation. Zn-*tri*-PcNc-8 sensitized TiO_2-based solar cell exhibited a maximum incident photo-to-current conversion efficiency (3.01%) in the red/near-IR light range (650-750 nm) without CDCA, which was much higher than that (1.96%) for a solar cell sensitized by Zn-*tri*-PcNc.[28-30]

In 2000, Cook *et al*. synthesized tribenzo[b,g,l]thiopheno-[3,4-q]porphyrazine and tribenzo[b,g,l] thiopheno[2,3-q]porphyrazine ring systems by cross cyclotetramerisation reactions of 3,6-dialkylphthalonitriles with 3,4-dicyanothiophene and 2,3-dicyanothiophene respectively, and tribenzo[b,g,l]thiopheno-[3,4-q]porphyrazine shows a strongly split Q-band absorption in the far red region of the spectrum and highly bathochromic shift relative to the corresponding band in symmetric phthalocyanine. On the other hand, their studies have indicated that 3,4-dicyanothiophene compared to phthalonitriles and 2,3-dicyanothiophene has lower reactivity in cross cyclotetramerisation reactions.[31] Subsequently Kimura and coworkers have synthesized bis(4-methylpyridine)-[1,3,5,7,9,11,13,15-octaphenyltetra(3,4-thieno)tetraazaporphy-rinato]ruthenium(II),[32] and Dubinina *et al.*[33] have investigated the characterization of binuclear thienoporphyrazines. Although the thiophene derivatives have been widely used in organic field-effect transistor (OFET) and organic photovoltaic (OPV) devices, the thiophene porphyrazines have not been noticed and applied in photocatalysis.

Herein we have synthesized a highly asymmetric and A_2BC type phthalocyanine derivatives (Zn-*di*-PhNcTh) using a carboxyl-naphthalene unit as electron acceptor and a diphenylphenoxy to retard the aggregation. Owing to the low reactivity and highly bathochromic shift of 3,4-dicyanothiophene, π electron rich thiophene ring has been in place of the benzenoid ring of phthalocyanine which was acting as an electron donor. By using this highly asymmetric A_2BC type phthalocyanine derivative as a sensitizer of g-C_3N_4, Zn-*di*-PcNcTh/g-C_3N_4 without CDCA coadsorbent exhibits a H_2 production efficiency of 249 μmol h^{-1} with an impressive turnover number (TON) of 9960.8 under visible light ($\lambda \geq 420$ nm) irradiation. Owing to the introduction of highly bathochromic shift of 3,4-dicyanothiophene, Zn-*di*-PcNcTh/g-C_3N_4 gives an extremely high apparent quantum yield (AQY) of 2.44%, 3.05%, 1.53% at 700, 730, 800 nm monochromatic light irradiation. The above results show the promising application of thiophene phthalocyanines in photocatalytic H_2 production system for more efficiently untilizing the solar radiation with wavelength from 600 nm to 800 nm.

Experimental

Dye synthesis

All chemicals were used as received unless otherwise stated. Butanol was freshly distilled from sodium, N,N-dimethylformamide (DMF) and dichloromethane (DCM) were distilled from CaH_2 under N_2. Thin layer chromatography (TLC) was performed on glass plates (20 cm × 20 cm) with GF-254 silica gel, and column chromatography was carried out on silica gel columns (Merk, Kieselgel60, 70-230mesh) with the appointed eluents. ^{1}H NMR (300 MHz) spectra were recorded on a Bruker DPX 300 spectrometer using solutions in deuterated solvents and tetramethylsilane (TMS) is the internal standard in NMR measurements. UV-vis spectra were obtained on a Hitachi U-4100 spectrophotometer. Fluorescence spectra were recorded with K2 ISIS spectrometer. IR spectra were recorded on a BIORAD FTS-165 spectrometer using KBr pellets. Matrix-assisted laser desorption/ionization time-of-flight mass spectrometry (MALDI-TOF-MS) was carried on a Bruker BIFLEX III ultrahigh resolution Fourier transform ion cyclotron resonance (FTICR) mass spectrometer using a-cyano-4-hydroxycinnamic acid as matrix. Elemental analyses were performed on a Vavio El III Elementar. The synthetic routes of 4,5-bis(2',6'-diphenylphenoxy)-phthalonitrile (ligand A), 3,4-dicyanothiophene (ligand B) and 6-Carboxymethyl-2,3-dicyanonaphthalene (ligand C) were shown in Supporting Information. 6-Carboxymethyl-2,3-dicyanonaphthalene were

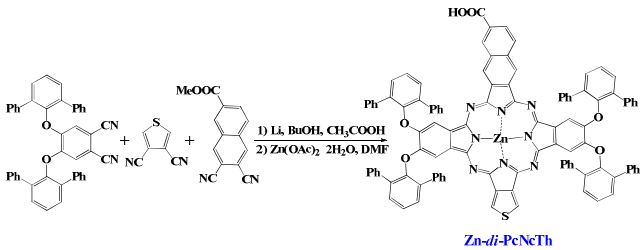

Scheme 1 Synthetic route of asymmetric Zn-*di*-PcNcTh.

View Article Online
DOI: 10.1039/C6DT01248E

prepared according to the previous methods.[28-30] The route to 4,5-bis(2',6'-diphenylphenoxy)-phthalonitrile has been described in earlier papers.[34,35] 3,4-Dicyanothiophene was prepared from commercially available 3,4-dibromothiophene by the Rosenmund von Braun reaction with copper(I) cyanide.[36, 37]

Synthesis of 8,9,24,25-tetra(2',6'-diphenylphenoxy)-16(or 17)-carboxyl zinc dibenzo naphthothiophenoporphyrazine (Zn-*di*-PhNcTh). A solution of 3,4-dicyanothiophene (136.1 mg, 1.02 mmol), 4,5-bis(2',6'-diphenylphenoxy)phthalonitrile (209.5 mg, 0.34 mmol) and 6-carboxymethyl-2,3-dicyanonaphthalene (120.4 mg, 0.51 mmol) in dry n-butanol (10 mL) was heated to 100 °C with stirring for 3 h. To the reactant mixture was added slowly lithium metal (0.2 g) under stirring (Scheme 1). The solution immediately turned an intense green color and was heated to reflux for 6 h. When the mixture was allowed to cool to room temperature, glacial acetic acid (10 mL) was added and stirring was continued at 70 °C for 30 min. The mixture was cooled to room temperature and methanol (100 mL) was added. Then the mixture was filtered and the precipitation was washed with methanol. The residue was separated by silica gel column chromatography with DCM as a solvent and monitored by UV-vis spectra. The component and properties of by-products were shown in Supporting Information.

The target product, 8,9,24,25-tetra(2',6'-diphenylphenoxy)-16(or 17)-carboxyl-30H,32H-dibenzonaphthothiophenoporphyrazine (H_2-*di(opp)*-PcNcTh) was separated by using DCM-MeOH (95:5) as eluent and recrystallized from DCM-MeOH to obtain a green solid. Yield: 10 mg, 3%. UV-vis λ_{max} (DCM)/nm (logε): 746 (4.74); 723 (4.90); 427 (4.32); 343 (4.71). ^{1}H NMR ($CDCl_3$, 300MHz): δ=8.14 (s, 2H，ThH), 7.89-7.74 (br, 48H, ArH), 6.98-6.89 ppm(br, 36H, ArH). FT-IR (KBr): ν (cm^{-1}) = 3292 (w, COOH), 3057 (w, ArCH), 3029 (w, ArCH), 1719 (w, C=O), 1617 (w, C=N), 1600, 1498, 1474, 1454, 1413, 1270, 1196, 1091, 1030, 880, 791, 751, 699 (Fig. S15†). TOF-MS (m/z): calcd for $C_{107}H_{66}N_8O_6S$ $[M+1]^+$ 1591.78; found 1591.27 (Fig. S21†); Elemental analysis calcd for $C_{107}H_{66}N_8O_6S{\cdot}CH_3OH{\cdot}CH_2Cl_2$: C 76.62, H 4.25, N 6.56; Found: C 76.07, H 4.69, N 6.22.

In a typical procedure, zinc acetate (68.0 mg, 0.314 mmol) was added to a stirred solution of H_2-*di(opp)*-PcNcTh (50 mg, 0.031 mmol) in DMF (20 mL) and heated to 100 °C for 8 h. The solvent was removed under reduced pressure and the residue was purified using column chromatography over silica gel and then recrystallized from DCM-MeOH to afford 8,9,24,25-tetra(2',6'-diphenylphenoxy)-16(or 17)-carboxyl-zinc-dibenzo-naphthothiophenoporphyrazine (Zn-*di*-PhNcTh) Yield: 48 mg, 92%. UV-vis λ_{max} (DCM)/nm (logε): 732 (5.13); 697 (4.96); 357 (4.81) (Fig. S1†). ^{1}H NMR ($CDCl_3$, 300MHz): δ=8.15 (s, 2H, ThH), 7.90-7.81 (br, 48H, ArH), 7.01-6.88 ppm(br, 36H, ArH) (Fig. S22†). FT-IR (KBr): ν (cm^{-1}) = 3292 (w, COOH), 3057 (w, ArCH), 3028 (w, ArCH), 1728 (w, C=O), 1612, 1500, 1454, 1413, 1268, 1197, 1092, 1028, 880, 750, 700 (Fig. S7†). TOF-MS (m/z) calcd for $ZnC_{107}H_{64}N_8O_6S$ $[M+1]^+$ 1653.40, found 1653.34 (Fig. S6†); Elemental analysis calcd for $ZnC_{107}H_{64}N_8O_6S{\cdot}CH_3OH$: C 79.98, H 4.23, N 6.91; Found: C 79.45, H 4.45, N 6.68.

Materials Preparation

Graphitic carbon nitride (g-C_3N_4) was synthesized by a simple thermolysis process of urea according to our previous report.[38] Typically, 5 g urea was placed in a closed crucible and calcinated at 580 °C for 3 h with a heating rate of 5 °C mim^{-1}, and then the yellow-colored product was washed by nitric acid (0.1 M) and distilled water, and then dried at 70 °C overnight to obtain the product (g-C_3N_4). Co-catalyst Pt nanoparticles were loaded on g-C_3N_4 by a photodeposition procedure. Typically, 0.2 g of g-C_3N_4 was suspended into 40 mL of water, 10 mL of methanol and 0.134 mL of H_2PtCl_6 (0.077 M) mixed solution, and then the suspension was irradiated using a 500 W high pressure Hg lamp for 3 h under stirring after dispersion in an ultrasonic bath for 10 min. The product was separated by centrifugation, washed with water, and then dried at 70 °C overnight to obtain 1.0 wt % Pt/g-C_3N_4.

Dye-sensitized g-C_3N_4 was prepared by an impregnation method. 0.1 g of Pt/g-C_3N_4 was dissolved with 3 mL of Zn-*di*-PcNcTh $CHCl_3$ solution (0.17 mM) under stirring for 12 h at 60 °C and then the product was filtered through a 0.45 μm nylon filter and dried at room temperature overnight. There was no signal of Zn-*di*-PcNcTh existence in the filtrate of the suspension after sensitization procedure, therefore the Zn-*di*-PcNcTh adsorbed amount on the calculated to be 5 μmol g^{-1}.

Electrochemical Measurement and Computational Details

Electrochemical measurements such as cyclic voltammetry (CV) were measured with a BAS CV-50W voltammetric analyzer, using a three-electrode cell with a glassy carbon disk working electrode, a silver-wire counter electrode, and a Ag/Ag^+ (0.01 M $AgNO_3$ in acetonitrile) reference electrode. The results were corrected for junction potentials using saturated calomel electrode (SCE) as typical units which have been referenced internally to the ferrocenium/ferrocene (Fc^+/Fc) couple [$E_{1/2}$(Fc^+/Fc) = 0.50 V vs. SCE]. Typically, a 0.1 M solution of $[Bu_4N][ClO_4]$ in DCM containing 0.5 mM ZnPc dye was purged with N_2 for 10 min, and the voltammogram was recorded at ambient temperature with a scan rate of 20 mV s^{-1}.

The primal input structures of Zn-*di*-PhNcTh were obtained by adding a benzene ring onto one of the benzene rings of phthalocyanine and then attaching six 2,6-diphenylphenoxy groups and one carboxyl group onto the peripheral positions. Moreover, a benzene ring of phthalocyanine was replaced by a π electron rich thiophene ring. The ground state geometries were optimized by using the B3LYP (BeckeLee-Young-Parr composite of exchange-correlation functional) method with the 6-31G(d) basis set, which has been proved to be suitable for calculating the molecular orbitals (MOs) of ZnPc derivatives. According to our previous reported method,[28-30] the hybrid density functional Becke-Lee-Young-Parr composite of exchange-correlation functional method was used for both geometry optimizations and property calculations. The Berny algorithm using redundant internal coordinates was employed in energy minimization and default cutoffs were used throughout. Electronic absorption spectroscopic calculations of H_2-*di(adj)*-PcNcTh and H_2-*di(opp)*-PcNcTh were made by TD-

View Article Online
DOI: 10.1039/C6DT01248E

DFT method on the basis of the optimized structures due to the large complex computation of Zinc phthalocyanine.[39] All calculations were carried out using the Gaussian 03 program in the IBM P690 system in High Performance Computing Center.[40]

Materials Characterization

UV-vis diffuse reflectance spectra (DRS) were obtained with a Shimadzu UV-3600 UV-vis-NIR spectrophotometer equipped with an integrating sphere. Photoluminescence (PL) spectra were determined by Hitachi F-4500 fluorescence spectrophotometer. Transient photocurrent was investigated on CHI 618C electrochemical analyzer with three-electrode system, where Pt wire, Pt plate and Ag/AgCl as work, counter and reference electrode, respectively. And the electrodes are immersed into a suspension containing 10 mg g-C_3N_4, Zn-*di*-PcNcTh-Pt/g-C_3N_4, 1.0 M NaOH and 5 mg methyl viologen (MV) as electron media, which was continuously purged by N_2 to remove O_2 before light irradiation.

Photocatalytic Property Tests

The H_2 production reaction was carried out in an outer irradiation-type photoreactor (Pyrex glass) connected to a closed gas-circulation system. A 300 W Xe-lamp (PLS-SXE300, Beijing Trusttech Co. Ltd., China) with an emission spectrum covering the whole UV-vis/IR region from 200 to > 1100 nm was used as the light source, and a cutoff filter ($\lambda \geq 420$ nm) was employed to obtain the visible-light irradiation. The H_2 evolution rate was analyzed with a gas chromatograph (GC, SP6890, TCD detector, 5 Å molecular sieve columns and Ar carrier). The photoreaction system contains 10 mg of Zn-*di*-PcNcTh /g-C_3N_4 as a photocatalyst, 10 mL of water, and 88 mg of ascorbic acid (AA, 50 mM) as an electron donor. The turnover number (TON) is usually defined by the number of reacted molecules and the number of active sites. In the present work, we assumed that H_2 production takes place when two electrons injected from the excited dye molecules react with two protons. One dye molecule can produce only one photogenerated electron which can be injected into the conduction band (CB) of g-C_3N_4, therefore two dye molecules are needed to react with two H^+ and produce one H_2 molecule. Apparent quantum yield (AQY) was measured under the same photoreaction condition but with monochromatic light irradiation obtained from band pass filter (for example, $\lambda = 700 \pm 10$ nm). The turnover number (TON) and apparent quantum yield (AQY) were calculated according to the following equations: [4,41]

$$\mathrm{TON}=\frac{2\times \text{ number of evolved } H_2 \text{ molecules}}{\text{Number of dye molecules adsorbed}} \quad (1)$$

$$\mathrm{AQY}(\%)=\frac{2\times \text{number of evolved } H_2 \text{ molecules}}{\text{Number of incident photons}}\times 100\% \quad (2)$$

Results and discussion

Dye syntheses and spectroscopic analyses

The target metal free phthalocyanine was prepared via cross cyclotetramerisation by using 6:2:3 of 3,4-dicyanothiophene, 4,5-bis(2',6'-diphenylphenoxy)-phthalonitrile and 6-carboxymethyl-2,3-dicyanonaphthalene with lithium n-butyloxide in n-butanol (Scheme 1). Owing to the lower reactivity of 3,4-dicyanothiophene compared to phthalonitriles, multitudinous 3,4-dicyanothiophene was added to limit the varieties of by-products.[31] A standard work-up included treatment with acetic acid to convert the initially formed lithium Pc derivatives into their corresponding metal-free products. The carboxymethyl ester was simultaneously hydrolyzed to carboxylic acid by lithium alkoxide base. It is noteworthy that purification of general phthalocyanine compounds has been a challenge for chemists, not to mention the separation of a series of closely related and isomeric phthalocyanines. Fortunately, the mixture could be separated into different fractions through silica gel column chromatography. There are tremendous discrepancy of the solubility and polarity of these phthalocyanine derivatives due to the difference of their molecule structure and symmetry. All of the five fractions give satisfactory C, H and N data, ^{1}H NMR spectra, MALDI-TOF-MS and IR spectra and the results are shown in the ESI†.

The highly asymmetric Zn-*di*-PcNcTh dye was characterized by elemental analysis, ^{1}H NMR, MALDI-TOF-MS, IR, UV-vis and fluorescence spectroscopy. The UV-vis absorption spectra (Fig. 1†) show that Zn-*di*-PcNcTh in DCM solution exhibits a strongly split Q absorption with a maximum absorption at 732 nm ($\varepsilon = 1.35 \times 10^5$ M^{-1} cm^{-1}) and submaximal absorption at 697 nm ($\varepsilon = 9.08 \times 10^4$ M^{-1} cm^{-1}), which was commonly in free metal phthalocyanines and asymmetric metal phthalocyanines.[31] Actually the reason of the splitting is the division of the LUMO due to the highly unsymmetrical of the molecular which can be proved in the computational section. The above data indicated Zn-*di*-PcNcTh which utilized a π electron rich thiophene ring in place of the benzenoid rings of phthalocyanine possesses a wilder and stronger optical absorption property and obvious red-shift of Q band than other phthalocyanine derivatives, which is favorable and significant for the visible/near-IR-light induced photocatalytic H_2 production. The fluorescence spectrum (Fig. S2†) of the asymmetric Zn-*di*-PcNcTh dye shows a maximum emission at 739 nm, and its optical energy gap (E_{0-0}) can be estimated to be 1.69 eV on the basis of the intersection point of the UV-vis absorption and fluorescence emission spectra as show in Fig. S2 in the ESI†.[21,41,42]

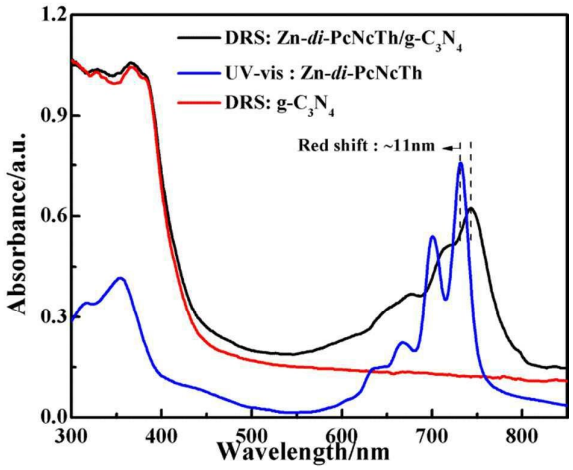

Fig. 1 UV-vis diffusion reflectance absorption spectra (DRS) of g-C_3N_4, Zn-*di*-PcNcTh/g-C_3N_4 and UV-vis absorption spectrum of Zn-*di*-PcNcTh solution.

View Article Online
DOI: 10.1039/C6DT01248E

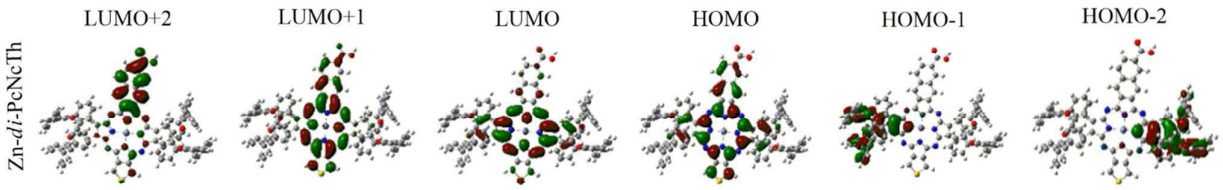

Fig. 2 The frontier molecular orbitals of Zn-*di*-PcNcTh, full optimized at B3LYP/6-31G level.

The IR spectrum (Fig. S7†) of Zn-*di*-PcNcTh shows obvious featured IR absorption bands of the central aromatic Pc macrocycle, such as the bands at 750-1750 cm^{-1} ascribable to the characteristic absorptions of Pc cores, the bands at 3057-3028 cm^{-1} ascribable to the aromatic C-H stretching vibrations, the bands at 1612 and 1500 cm^{-1} ascribable to the aromatic C=C stretching vibrations, the band at ~ 1000 cm^{-1} due to the aromatic in-plane C-H vibrations, and the bands at 1439-1454 cm^{-1} and 1312-1323 cm^{-1} ascribable to the stretching vibrations of isoindole and pyrrole rings, respectively. Moreover, the intense absorptions at 1728 cm^{-1} can be attributed to the stretching vibrations of -COOH in the asymmetric Zn-*di*-PcNcTh. As can be seen from the FTIR spectra in Fig. S8 in the ESI†, the pristine g-C_3N_4 exhibits characteristic IR absorption peaks similar to that in the previous literature.[4,41] The four strong peaks at 1238, 1317, 1407, and 1573 cm^{-1} can be ascribed to the CN heterocycle stretching of g-C_3N_4, while the absorption band 1640 cm^{-1} can be ascribed to the C-N stretching vibration, and a shoulder broad band near 3166 cm^{-1} corresponds to the stretching mode of terminal –NH groups at the defect sites of the aromatic ring.[4] The FTIR spectra of the Zn-*di*-PcNcTh/g-C_3N_4 (either with 2.5 or even 10 μmol g^{-1} dye-adsorbed amount) are similar to the IR absorption peak positions as that of the pristine g-C_3N_4, due to the weak IR absorption peak positions of Zn-*di*-PcNcTh are covered in the FTIR spectra of the pristine g-C_3N_4. UV-vis diffuse reflectance absorption spectra of g-C_3N_4, Zn-*di*-PcNcTh/g-C_3N_4 are also listed in Fig. 1. After adsorbing on Pt/g-C_3N_4, intense red/near-IR adsorption band similar to the corresponding dye solution can also be observed. Moreover, Zn-*di*-Pc-NcTh/g-C_3N_4 show much broader red/near-IR light absorption from 550 to 850 nm than the pristine g-C_3N_4, which just absorbs light with wavelength shorter than 450 nm due to the rather large bandgap (~ 2.70 eV).[8] Simultaneously, the maximal absorption wavelengths of Zn-*di*-PcNcTh/g-C_3N_4 exhibit about ~ 11 nm red-shift as compared to Zn-*di*-PcNcTh solution, which may be caused by the efficient interaction between Zn-*di*-PcNcTh and g-C_3N_4. The other characterization results such as elemental analyses, ^{1}H NMR and MS spectra were also obtained for Zn-*di*-PcNcTh as shown in the ESI.†

Dye electrochemical analyses

The electrochemical behavior of Zn-*di*-PcNcTh was investigated by cyclic voltammetry (CV) in DCM solution (Fig. S9†).The first half-wave redox potential values (vs. SCE) are summarized in Table 1. E_{ox} (vs SCE) = E_{ox} (vs Ag/$AgNO_3$) – $E_{1/2}$ (Fc^+/Fc vs Ag/$AgNO_3$) + $E_{1/2}$ (Fc^+/Fc vs SCE).[43,44] As can be seen, the highest occupied molecular orbital (HOMO, E_{ox}) of dye can be obtained by curves and the lowest unoccupied molecular orbital (LUMO) can be calculated by $E^* = E_{ox} - E_{0\text{-}0}$, where $E_{0\text{-}0}$ (= $1240/\lambda_{intersection}$) is obtained by the intersection point of the normalized absorption and emission spectra as shown in Fig. S2,† and therefore E^* (E_{LUMO}) of Zn-*di*-PcNcTh can be estimated to be -1.39 eV (vs. SCE) as shown in Table 1. The LUMO levels is sufficiently negative than the CB level (-1.12 eV)[7,45] of g-C_3N_4, indicating that the photogenerated electrons of the excited dye can availably inject into the conduction band (CB) of g-C_3N_4 on aspect of thermodynamics

Density functional theory calculations

The UV-vis absorption spectra of H_2-*di(adj)*-PcNcTh and H_2-*di(opp)*-PcNcTh were calculated using the TD-DFT method based on the optimized structures. The calculated electronic absorption spectra of self-assembled donor-acceptor dyads H_2-*di(adj)*-PcNcTh and H_2-*di(opp)*-PcNcTh are shown in Fig. S3.† The H_2-*di(opp)*-PcNcTh have two split Q absorption bands which are 696 nm and 652 nm and H_2-*di(adj)*-PcNcTh have more split Q absorption bands at 721, 615, 611 and 607 nm. The calculated energy splitting between the Q bands for H_2-*di(adj)*-PcNcTh is significantly larger than that for H_2-*di(opp)*-PcNcTh, which is corresponding with UV-vis absorption spectra feature in Fig. S4.† As can be seen, the maxium absorption peak of the Q band of H_2-*di(adj)*-PcNcTh is at 757 nm and 722 nm for H_2-*di(opp)*-PcNcTh. It is evident that the Q absorption bands of H_2-*di(adj)*-PcNcTh are red-shifted compared with H_2-*di(opp)*-PcNcTh, which corresponds well with its smaller HOMO-LUMO gap (Fig. S5†). On the other hand, the Q band of H_2-*di(adj)*-PcNcTh spilts at 757 nm and 671 nm and the spilt of the Q band of H_2-*di(opp)*-PcNcTh is not obvious, which is in accordance with their calculated electronic absorption spectra. The UV-vis absorption spectra of substituted H_2-*di(adj)*-PcNcTh and H_2-*di(opp)*-PcNcTh complexes have many differences, indicating that the two 4,5-bis(2',6'-diphenylphenoxy)phthalonitrile are adjacent and opposite which affect the molecular orbitals of the ring to different extents. So we can distinguish H_2-*di(adj)*-PcNcTh and H_2-*di(opp)*-PcNcTh through their different UV-vis absorption spectra. In addition, the major product is H_2-*di(opp)*-PcNcTh, owing to the big steric hindrance of 4,5-bis(2',6'-diphenylphenoxy)phthalonitrile, H_2-*di(opp)*-PcNcTh is more stable than H_2-*di(adj)*-PcNcTh.

Density functional theory (DFT) calculations were performed on Zn-*di*-PcNcTh at the B3LYP/6-31G(d) level, which has been proved to be suitable for calculating the MOs of ZnPc derivatives. As shown

Table 1. Optical and electrochemical data and band positions of Zn-*di*-PcNcTh

Dye	λ_{max} / nm	ε /×10^4 M^{-1} cm^{-1}	E_{ox} / V *vs*. SCE	E_{red} / V *vs*. SCE	$E_{0\text{-}0}$ /eV	E^*[a]/ eV
Zn-*di*-PcNcTh	732	13.5	0.30(Oxd_1)	-0.98(Red_1)	1.69	-1.39

[a]Calculated with the formula $E^*=E_{ox} - E_{0\text{-}0}$.

View Article Online
DOI: 10.1039/C6DT01248E

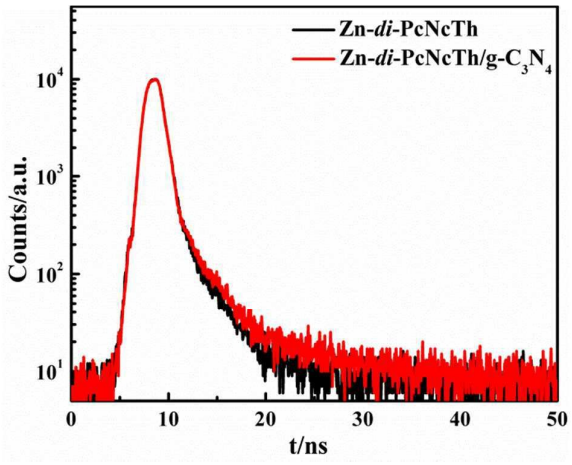

Fig. 3 Time-resolved fluorescence decay curves of Zn-*di*-PcNcTh and Zn-*di*-PcNcTh/g-C_3N_4 films.

in Fig. 2, the electron density of Zn-*di*-PcNcTh for HOMO-1 and HOMO-2 are shared by the 2,6-diphenylphenoxy donor moiety. The HOMO of Zn-*di*-PcNcTh is delocalized over the entire molecule. The LUMO+1 and LUMO are π* orbitals delocalized across the Pc ring moving to the carboxyl group, while the LUMO+2 is mainly localized over the naphthalene ring and the carboxyl group. This indicates that the photoexcited electrons can effectively transfer from the Pc skeleton to the carboxyl group, which is beneficial for the injection of the photoexcited electrons to the g-C_3N_4 CB during photocatalytic H_2 producton operation.

Fluorescence spectra analyses

The photoluminescence (PL) spectrum is an effective method to investigate the electron transfer behavior between dye and semiconductor.[16,46,47] As the results in Fig. S10† show, Zn-*di*-PcNcTh solution exhibits intense emission bands centered at around 739 nm with excitation wavelength of 666 nm. It indicates that the strong recombination process of the photogenerated electron-hole pair of the excited dye. However, obvious quenching effect can be observed when g-C_3N_4 is added into the dye solutions, implying the rapid electron transfer from the excited dye molecules to CB of g-C_3N_4 since there is no overlap between the absorption spectra of g-C_3N_4 and emission spectra of Zn-*di*-PcNcTh.[47]

Time-resolved fluorescence spectra (TRPS) is an efficient method to investigate the recombination rate of the photogenerated electron-hole pairs, and the corresponding fluorescence lifetime (t) represents the average existence time of excited dye molecules. The effects of Pt/g-C_3N_4 on the fluorescence lifetime of the excited Zn-*di*-PcNcTh are shown in Fig. 3 and Table 2. The fluorescence lifetimes of the systems are obtained by fitting the time-resolved fluorescence decay curves with the following exponential fitting equation.

Table 2. Time-resolved fluorescence decay data of Zn-*di*-PcNcTh and Zn-*di*-PcNcTh/g-C_3N_4 films derived from Fig. 3

System	τ_f / ns	χ^2	λ_{detet} /nm
Zn-*di*-PcNcTh	2.29	0.977	740
Zn-*di*-PcNcTh/g-C_3N_4	2.44	0.983	740

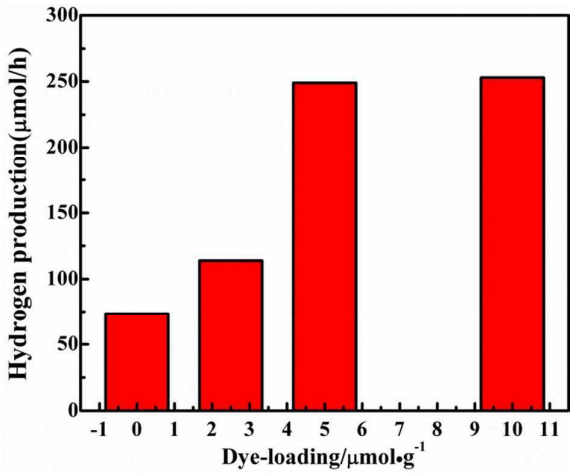

Fig. 4 Effect of Zn-*di*-PcNcTh amount on the photoactivity for H_2 production over Zn-*di*-PcNcTh/g-C_3N_4. The conditions are as follows: 10 mg of 1.0 wt% Pt-loaded catalyst with 10 mL of water containing 50 mM AA and without adding CDCA under λ ≥ 420 nm light irradiation.

$$\text{Fit} = A + B_1 \exp\left(-\frac{t}{\tau_1}\right) + B_2 \exp\left(-\frac{t}{\tau_2}\right) + B_3 \exp\left(-\frac{t}{\tau_3}\right) \quad (3)$$

where A, B_1, B_2 and B_3 are constants and obtained after fitted every decay curves. As can be seen from Table 2, the fluorescence lifetime (τ) of Zn-*di*-PcNcTh is delayed from 2.29 ns to 2.44 ns, the lifetime enhancement is 70% when Pt/g-C_3N_4 is added, indicating that the photogenerated carrier recombination of Zn-*di*-PcNcTh is strongly restrained due to the efficient electron transfer from the excited Zn-*di*-PcNcTh to g-C_3N_4.

Photocatalytic activity analyses of Zn-*di*-PcNcTh/g-C_3N_4

Photocatalytic H_2 production reaction of a dye-sensitized Pt/g- C_3N_4 photocatalytic system is usually affected by series of conditions such as electron donors, co-catalyst Pt, irradiation wavelength and time, dye-adsorbed amount and so on.[23] The prsent system adopts the photoreaction condition similar to our previous report by considering the similarity in the photocatalytic system.[4,38, 41,45]

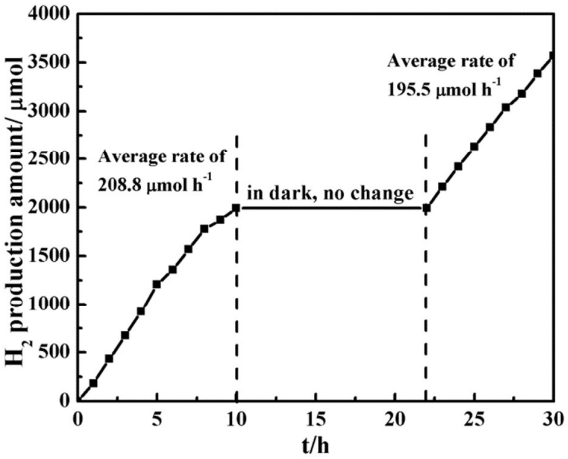

Fig. 5 Long-term stability for H_2 production of Zn-*di*-PcNcTh/g-C_3N_4 without adding coadsorbent CDCA under λ ≥ 420 nm light irradiation.

View Article Online
DOI: 10.1039/C6DT01248E

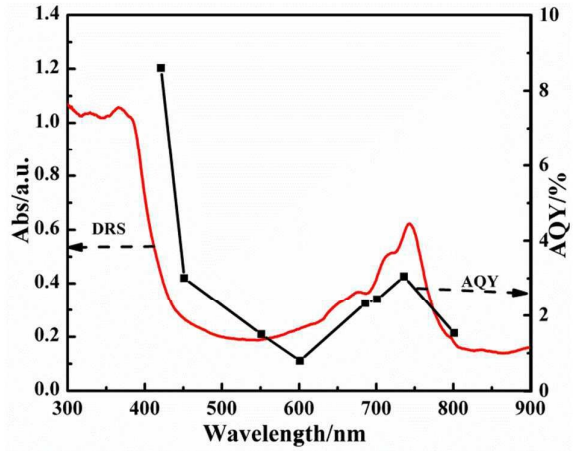

Fig. 6 Comparison of DRS spectra and AQY values of Zn-*di*-PcNcTh/g-C_3N_4 under optimal photoreaction conditions and different monochromatic light irradiation.

Ascorbic acid (AA) as sacrificial reagent and $\lambda \geq 420$ nm light irradiation are used to further optimize the photoreaction condition of Zn-*di*-PcNcTh/g-C_3N_4 and the corresponding results are shown in Fig. 4. The H_2 production efficiency of Zn-*di*-PcNcTh/g-C_3N_4 at $\lambda \geq 420$ nm light irradiation are similar to that under $\lambda \geq 500$ nm light irradiation with AA as sacrificial reagent.[4] As can be seen, optimal photoreaction conditions would be: 10 mg 1.0 wt % Pt-loaded g-C_3N_4 sensitized with Zn-*di*-PcNcTh dye, dispersed in 50 mM AA water solution (10 mL). In addition to the above conditions, the dye absorbed amount have been studied. As light harvester and photoelectron generator, Zn-*di*-PcNcTh plays the major role in a dye sensitized photocatalytic system. As Fig. 4 shown, the photocatalytic H_2 production rate is improved dramatically by increasing adsorbed amount of Zn-*di*-PcNcTh. However, the photoactivity remained stable when the adsorbed amount of Zn-*di*-PcNcTh exceeded 5.0 μmol g^{-1}. This phenomenon should be reasonable in terms of the competitive relation between light harvesting and active sites for H_2 production. On the other hand, CDCA as a coadsorbent which reduces the dye aggregation, is commonly used in ZnPc-sensitized solar cells to improve cell performance. However, some ZnPc derivatives with large steric hindrance by introducing bulky diphenylphenoxy substitutions can effectively retard ZnPc molecular aggregates. Zn-*di*-PcNcTh with four diphenylphenoxy substitutions also can effectively suppress molecular aggregates, then an impressive photocatalytic H_2 production rate was obtained without adding CDCA.

The transient photocurrent behavior of Zn-*di*-PcNcTh-sensitized g-C_3N_4 suspension under $\lambda \geq 420$ nm light irradiation are shown in Fig. S11.† It is evident that the dye-sensitized g-C_3N_4 exhibits higher photocurrent than g-C_3N_4, illustrating the effective and fast electron transfer from Zn-*di*-PcNcTh to g-C_3N_4. Fig. 5 depicts the long-term photostability for H_2 production of Zn-*di*-PcNcTh/g-C_3N_4 system without adding CDCA under the above-mentioned conditions. As can be seen, Zn-*di*-PcNcTh/g-C_3N_4 shows excellent photoactivity and rather good stability for H_2 production under $\lambda \geq 420$ nm light irradiation. The average H_2 production efficiency is 208.8 μmol h^{-1} in the first 10 h and 195.5 μmol h^{-1} in the second 10 h. Although the photoactivity have decreased to some extent during a second 10 h irradiation after remaining in darkness overnight, it still can be concluded that the present Zn-*di*-PcNcTh/g-C_3N_4 leads to efficient utilization of near-IR light. Zn-*di*-PcNcTh after 10 h of light irradiation shows an absorption property and peak position very similar to that without irradiation, and there is no absorption signal of Zn-*di*-PcNcTh in the filtrate of Zn-*di*-PcNcTh/g-C_3N_4 suspension after 10 h of light irradiation, as shown in Fig. S12a.† The above results indicate that the Zn-*di*-PcNcTh molecule stay the same after prolonged use and no Zn-*di*-PcNcTh molecule desorbed from g-C_3N_4. Those desorbed Zn-*di*-PcNcTh with/without 10 h of irradiation, which are obtained by a desorption procedure (namely, catalyst was dispersed in 0.2 M KOH in ethanol/THF/water (2:2:1) solution several times, and the liquid supernatant and precipitate were collected), also show DRS spectra very similar to the original one, as can be seen from Fig. S12b.†

The photocatalytic H_2 production amount over photocatalyst is also measured under various monochromatic light irradiation with λ = 420, 450, 550, 600, 685, 700, 735 and 800 nm, using corresponding narrow band-pass filters, and then the wavelength-dependent AQY values are calculated based on the H_2 production rate and corresponding incident monochromatic light intensity according to equation 2 which has been shown in experimental section. The results in Fig. 6 show the comparison of the DRS spectra and AQY values as a function of the incident monochromatic light wavelength of g-C_3N_4 and Zn-*di*-PcNcTh/g-C_3N_4 without coadsorption of CDCA. It is evident that AQY values of Zn-*di*-PcNcTh/g-C_3N_4 correspond with its DRS spectrum. It is worthy of mention that Zn-*di*-PcNcTh/g-C_3N_4 shows considerably good AQY values of 2.44%, 3.02% under 700 and 735 nm monochromatic light irradiation, respectively. This result indicates that Zn-*di*-PcNcTh is an efficient dye for g-C_3N_4 photoactivity H_2 production.

Conclusions

A novel highly asymmetric zinc phthalocyanine derivative (Zn-*di*-PcNcTh) containing a π electron rich thiophene ring acting as electron donor, a carboxyl-naphthalene unit as electron acceptor and diphenylphenoxy to retard the aggregation has been successfully synthesized for developing red/near-IR responsive dyes of Pt-loaded graphitic carbon nitride for photocatalytic H_2 production. Ultraviolet-visible light (UV-vis), diffuse reflectance absorption spectra (DRS), photoluminescence (PL) spectra, time-resolved photoluminescence spectra (TRPS), and energy band structure analyses are adopted to investigate the photogenerated electron transfer process between Zn-*di*-PcNcTh and g-C_3N_4. After optimizing the photocatalytic condition Zn-*di*-PcNcTh sensitized g-C_3N_4 photocatalyst shows a H_2 production efficiency of 249 μmol h^{-1} under visible/near-IR-light irradiation without adding CDCA, corresponding to a TON of 9960.8 h^{-1}. Zn-*di*-PcNcTh/g-C_3N_4 gives an extremely high apparent quantum yield (AQY) of 2.44%, 3.05%, 1.53% at 700, 730, 800 nm monochromatic light irradiation.

Acknowledgements

This work is supported by the Natural Science Foundation of China (21573166, 21271146, 21271144, and 20973128), the

View Article Online
DOI: 10.1039/C6DT01248E

Funds for Creative Research Groups of Hubei Province (2014CFA007) and Natural Science Foundation of Jiangsu Province (SBK2015020824).

Notes and references

1 A. Kubacka, M. Fernandez-Garcia and G. Colon, *Chem. Rev.*, 2012, **112**, 1555-1614.
2 Y. Qu and X. Duan, *Chem. Soc. Rev.*, 2013, **42**, 2568-2580.
3 K. S. Joya, Y. F. Joya, K. Ocakoglu and R. van de Krol, *Angew. Chem. Int. Ed.*, 2013, **52**, 10426-10437.
4 X. Zhang, L. Yu, C. Zhuang, T. Peng, R. Li and X. Li, *ACS Catal.*, 2014, **4**, 162-170.
5 J. Zhu, P. Xiao, H. Li and S. A. C. Carabineiro, *ACS Appl. Mater. Interfaces*, 2014, **6**, 16449-16465.
6 X. Wang, S. Blechert and M. Antonietti, *ACS Catal.*, 2012, **2**, 1596-1606.
7 H. Yan and Y. Huang, *Chem. Commun.*, 2011, **47**, 4168-4170.
8 X. Zhang, B. Peng, S. Zhang and T. Peng, *ACS Sustainable Chem. Eng.*, 2015, **3**, 1501-1509.
9 X. Fan, L. Zhang, R. Cheng, M. Wang, M. Li, Y. Zhou and J. Shi, *ACS Catal.*, 2015, **5**, 5008-5015.
10 S. Cao and J. Yu, *J. Phys. Chem. Lett.*, 2014, **5**, 2101-2107.
11 Y. Ye, N. D. Ball, J. W. Kampf and M. S. Sanford, *J. Am. Chem. Soc.*, 2010, **132**, 14682-14687.
12 J. Zhang, X. Chen, K. Takanabe, K. Maeda, K. Domen, J. D. Epping, X. Fu, M. Antonietti and X. Wang, *Angew. Chem. Int. Ed.*, 2010, **49**, 441-444..
13 Y. Di, X. Wang, A. Thomas and M. Antonietti, *ChemCatChem*, 2010, **2**, 834-838.
14 J. Liu, Y. Zhang, L. Lu, G. Wu and W. Chen, *Chem. Commun.*, 2012, **48**, 8826-8828.
15 K. Takanabe, K. Kamata, X. Wang, M. Antonietti, J. Kubota and K. Domen, *Phys. Chem. Chem. Phys.*, 2010, **12**, 13020-13025.
16 S. Min and G. Lu, *J. Phys. Chem. C*, 2012, **116**, 19644-19652.
17 J. Xu, Y. Li, S. Peng, G. Lu and S. Li, *Phys. Chem. Chem. Phys.*, 2013, **15**, 7657-7665.
18 T. T. Le, M. S. Akhtar, D. M. Park, J. C. Lee and O. B. Yang, *Appl. Catal., B* 2012, **111-112**, 397-401.
19 R. Abe, K. Shinmei, K. Hara and B. Ohtani, *Chem. Commun.*, 2009, 3577-3579.
20 R. Abe, K. Shinmei, N. Koumura, K. Hara and B. Ohtani, *J. Am. Chem. Soc.*, 2013, **135**, 16872-16884.
21 X. Zhang, U. Veikko, J. Mao, P. Cai and T. Peng, *Chemistry*, 2012, **18**, 12103-12111.
22 S. A. Berhe, Z. B. Molinets, M. N. Frodeman, B. Miller, V. N. Nesterov, K. M. Haynes, C. M. Perry, M. T. Rodriguez, R. N. McDougald and W. J. Youngblood, *J. Porphyrins Phthalocyanines*, 2015, **19**, 1021-1031.
23 X. Chen, S. Shen, L. Guo and S. S. Mao, *Chem. Rev.*, 2010, **110**, 6503-6570.
24 X. Zhang, L. Yu, C. Zhuang, T. Peng, R. Li and X. Li, *RSC Adv.*, 2013, **3**, 14363.
25 Y. Zhang, F. Mao, H. Yan, K. Liu, H. Cao, J. Wu and D. Xiao, *J. Mater. Chem. A*, 2015, **3**, 109-115.
26 Y. Wang, J. Hong, W. Zhang and R. Xu, *Catal. Sci. Technol.*, 2013, **3**, 1703-1711.
27 D. Wang, J. Huang, X. Li, P. Yang, Y. Du, C. M. Goh and C. Lu, *J. Mater. Chem. A*, 2015, **3**, 4195-4202.
28 L. Yu, W. Shi, L. Lin, Y. Guo, R. Li and T. Peng, *Dyes and Pigments*, 2015, **114**, 231-238.
29 L. Lin, B. Peng, W. Shi, Y. Guo and R. Li, *Dalton Trans.*, 2015, **44**, 5867-5874.
30 L. Yu, X. Zhou, Y. Yin, Y. Liu, R. Li and T. Peng, *ChemPlusChem*, 2012, **77**, 1022-1027.
31 M. J. Cook and A. Jafari-Fini, *Tetrahedron*, 2000, **56**, 4085-4094.
32 T. Kimura, T. Iwama, T. Namauo, E. Suzuki, T. Fukuda, N. Kobayashi, T. Sasamori and N. Tokitoh, *Eur. J. Inorg. Chem.*, 2011, **2011**, 888-894.
33 T. V. Dubinina, N. E. Borisova, M. V. Sedova, L. G. Tomilova, T. Furuyama and N. Kobayashi, *Dyes and Pigments*, 2015, **117**, 1-6.
34 S. Mori, M. Nagata, Y. Nakahata, K. Yasuta, R. Goto, M. Kimura and M. Taya, *J. Am. Chem. Soc.*, 2010, **132**, 4054-4055.
35 M. E. Ragoussi, J. J. Cid, J. H. Yum, G. de la Torre, D. Di Censo, M. Gratzel, M. K. Nazeeruddin and T. Torres, *Angew. Chem. Int. Ed.*, 2012, **51**, 4375-4378.
36 C. B. Nielsen and T. Bjørnholm, *Org. Lett.*, 2004, **6**, 3381-3384.
37 A. Saeki, S. Yoshikawa, M. Tsuji, Y. Koizumi, M. Ide, C. Vijayakumar and S. Seki, *J. Am. Chem. Soc.*, 2012, **134**, 19035-19042.
38 X. Zhang, T. Peng, L. Yu, R. Li, Q. Li and Z. Li, *ACS Catal.*, 2015, **5**, 504-510.
39 L. Yu, L. Lin, Y. Liu and R. Li, *J. Mol. Graph. Model.*, 2015, **59**, 100-106.
40 R. Li, D. Qi, J. Jiang and Y. Bian, *J. Porphyrins Phthalocyanines*, 2010, **14**, 421-437.
41 L. Yu, X. Zhang, C. Zhuang, L. Lin, R. Li and T. Peng, *Phys. Chem. Chem. Phys.*, 2014, **16**, 4106-4114.
42 K. Kilså, E. I. Mayo, B. S. Brunschwig, H. B. Gray, N. S. Lewis and J. R. Winkler, *J. Phys. Chem. B*, 2004, **108**, 15640-15651.
43 Y. Zhang, P. Ma, P. Zhu, X. Zhang, Y. Gao, D. Qi, Y. Bian, N. Kobayashi and J. Jiang, *J. Mater. Chem.*, 2011, **21**, 6515-6524.
44 J. He, G. Benkö, F. Korodi, T. Polívka, R. Lomoth, B. Åkermark, L. Sun, A. Hagfeldt and V. Sundström, *J. Am. Chem. Soc.*, 2002, **124**, 4922-4932.
45 X. Zhang, L. Yu, R. Li, T. Peng and X. Li, *Catal. Sci. Technol.*, 2014, **4**, 3251-3260.
46 M. Zhu, Z. Li, B. Xiao, Y. Lu, Y. Du, P. Yang and X. Wang, *ACS Appl. Mater. Interfaces*, 2013, **5**, 1732-1740.
47 Y. Liu, C.-Y. Liu and Y. Liu, *Applied Surface Science*, 2011, **257**, 5513-5518.